iScience

CellPress
OPEN ACCESS

Perspective

In vivo super-resolution of the brain – How to visualize the hidden nanoplasticity?

Katrin I. Willig[1,*]

SUMMARY

Super-resolution fluorescence microscopy has entered most biological laboratories worldwide and its benefit is undisputable. Its application to brain imaging, for example in living mice, enables the study of sub-cellular structural plasticity and brain function directly in a living mammal. The demands of brain imaging on the different super-resolution microscopy techniques (STED, RESOLFT, SIM, ISM) and labeling strategies are discussed here as well as the challenges of the required cranial window preparation. Applications of super-resolution in the anesthetized mouse brain enlighten the stability and plasticity of synaptic nanostructures. These studies show the potential of *in vivo* super-resolution imaging and justify its application more widely *in vivo* to investigate the role of nanostructures in memory and learning.

INTRODUCTION

With the pioneering work on two-photon excitation (2PE) microscopy by Denk, Strickler, and Webb in 1990, it became possible to image deep in living tissue with sub-cellular resolution (Denk et al., 1990; Svoboda and Yasuda, 2006). Together with the advent of genetically encoded fluorescent proteins, this marks a turning point in brain research: It became possible to study cellular processes of brain function in their natural habitat, the intact brain. Such studies on living animals are particularly useful in the context of learning and memory. Early *in vivo* studies, for example, have demonstrated that pre- and postsynaptic elements such as axonal boutons and dendritic spines are highly volatile and undergo extensive elimination and formation (De Paola et al., 2006; Holtmaat et al., 2005). It is still debated as to where the locus for memory formation is, either in the activity pattern of the neuronal networks and/or the plasticity of single synapses (Langille and Brown, 2018). However, details of sub-cellular structural plasticity of synaptic proteins and receptors in the *in vivo* context are largely unknown owing to the limited spatial resolution of light microscopy. The resolution of a conventional light microscope is often estimated by the full width at half maximum (FWHM) of the pointspread function (PSF), which is the smallest spreading to which light can be focused. Its FWHM is $\sim \lambda/2NA$, with NA denoting the numerical aperture of the objective lens and λ the wavelength. Thus, far-field light microscopy is limited to a resolution of ~200 nm. This limit is overcome by super-resolution microscopy techniques, which are now widely used to study fixed and living cells (Eggeling et al., 2015; Sahl et al., 2019; Sheppard, 2021a).

This review focuses on super-resolution microscopy techniques that have been applied *in vivo* in the mouse brain or offer a strong potential for *in vivo* usability. The basic requirements for *in vivo* applicability are similar to live cell imaging and encompass fast image recording capability, live cell compatible fluorescence labeling, and low phototoxicity. Key to the application of super-resolution *in vivo*, however, is the possibility to acquire images within densely labeled tissue, and therefore requires an optical sectioning capability. This is usually not a feature of the super-resolution method itself, but a result of a combination of the super-resolution technique with traditional methods for optical sectioning. Under these aspects, we discuss linear structured illumination microscopy (SIM) and image scanning microscopy with pixel reassignment; both improve the resolution by a factor of two at the most. Theoretically unlimited *in vivo* super-resolution methods discussed here encompass stimulated emission depletion (STED), either with one or two photon excitation, and reversible saturable optical fluorescence transitions (RESOLFT) microscopy. For all super-resolution *in vivo* applications, there is a large demand for labeling techniques of endogenous proteins that are compatible *in vivo*, that do not interfere with protein function, and are bright and photostable.

[1]Group of Optical Nanoscopy in Neuroscience, Max Planck Institute for Multidisciplinary Sciences, City Campus, Göttingen, Germany

*Correspondence: kwillig@mpinat.mpg.de

https://doi.org/10.1016/j.isci.2022.104961

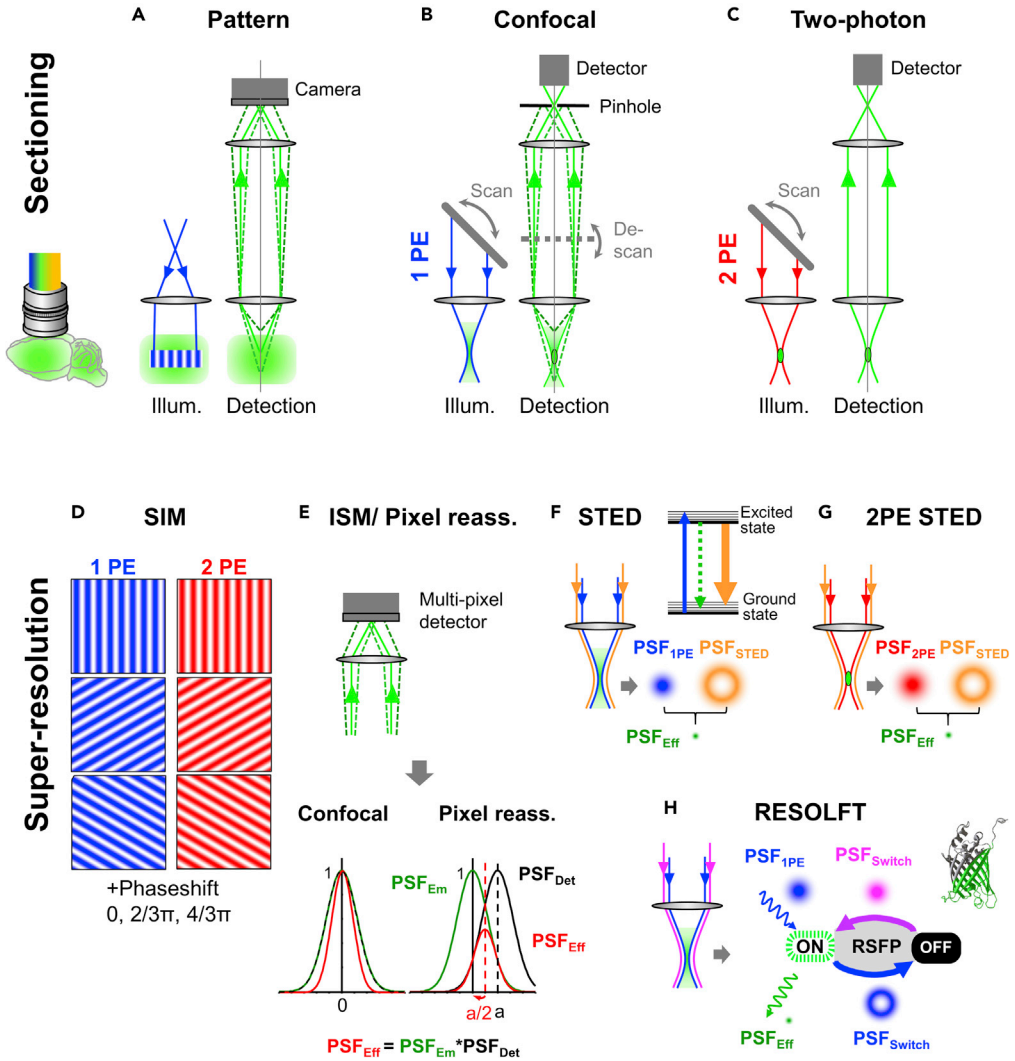

Figure 1. Methods of sectioning capability in far-field light microscopy and super-resolution techniques that can be combined for *in vivo* or deep tissue imaging

(A–C) Optical sectioning by wide-field imaging with patterned illumination (A), scanning confocal (B), and two-photon imaging (C).

(D and E) Restricted super-resolution by factor of two resolution improvement over conventional wide-field imaging by structured illumination (SIM) (D) or image scanning microscopy (ISM) together with pixel reassignment (E).

(F–H) Theoretically unlimited super-resolution by STED microscopy with one-photon excitation (1PE) (F), Two-photon excitation (2PE) STED microscopy (G), and RESOLFT microscopy (H). PSF: pointspread function.

SUPER-RESOLUTION TECHNIQUES FOR *IN VIVO* BRAIN IMAGING

Structured illumination microscopy

The principle of SIM microscopy states that spatial frequencies that are too high to be transmitted to the detector can be down-shifted by patterned illumination (Lukosz and Marchand, 1963). When the illumination of a certain pattern frequency mixes with the spatial frequencies of the label distribution in the sample, lower effective signal frequencies are generated, which are able to pass through the imaging lenses to the detector (For review see (Sheppard, 2021a; Zheng et al., 2021)). The practical implementation of SIM for fluorescence imaging was mainly driven by Gustafsson et al. (Gustafsson, 2000); by illuminating with a sinusoidal pattern at three different orientations and three different offsets of the stripes fluorescence images could be reconstructed with twice the conventional resolution (Figure 1D). As the fluorescence signal is detected with a camera, the question arises whether this technique is suitable for imaging thick and densely labeled tissue. Interestingly, such a patterned illumination can also be employed to achieve optical

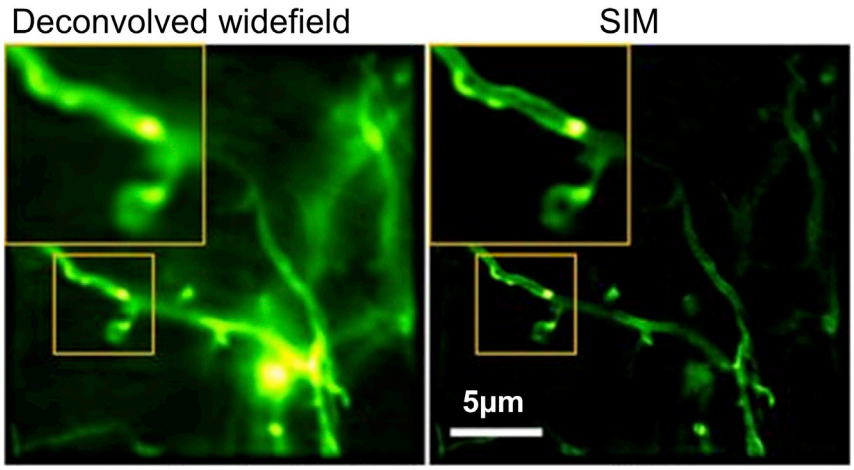

Figure 2. *In vivo* structured illumination microscopy (SIM) and corresponding de-convolved wide field image of the mouse cortex

The membrane of dendrites is labeled with ChR2-GFP. Optical aberrations are corrected by adaptive optics; image acquisition and reconstruction are specifically adapted to *in vivo* conditions. Adapted from (Turcotte et al., 2019).

sectioning in wide-field microscopes (Figure 1A). Neil et al. have shown a method to project a grid onto the focal plane to illuminate the object with a sinusoidal pattern (Neil et al., 1997, 1998). In this manner, three images are recorded of the same grid orientation but with different offsets. A reconstruction by a simple non-linear algorithm discards unmodulated out-of-focus light and produces optical sectioning, although without improving the lateral resolution. Very recently, the group of Na Ji improved this method by developing a better reconstruction algorithm and incorporating adaptive optics (Li et al., 2020). They called this method optical-sectioning structured illumination microscopy (OS-SIM) and applied it for *in vivo* imaging of the mouse cortex, zebrafish larval motor neurons and performed functional imaging. To achieve a resolution improvement, however, additional images at different illumination orientations are required, as performed in SIM. Unfortunately, the term SIM is used very general and includes any kind of illumination patterns such as stripes or the point illumination in a confocal microscope (Sheppard, 2021a). In the following, the term SIM will be used only for reconstructions from stripe patterns with a factor two of resolution improvement for which it is most widely used.

In recent years, SIM evolved to become an attractive choice for live-cell imaging. It is able to super-resolve also in three-dimensions (Gustafsson et al., 2008) and, by non-linear saturation of the excited state, the resolution can be improved by more than a factor of two (Gustafsson, 2005). The image acquisition is extremely fast with up to 400 frames per second (Kner et al., 2009; Li et al., 2015) and a fast reconstruction algorithm allows the real-time display of multi-color SIM data at video rate (Markwirth et al., 2019). Moreover, SIM requires no special fluorophores and the light levels without saturated excitation are relatively low. This gives the impression that SIM may be an attractive choice for *in vivo* imaging. On the other hand, *in vivo* imaging poses several challenges for a wide-field-based technique owing to potential motion artifacts attributable to vital functions. This was overcome by the groups of Na Ji and Eric Betzig that have applied SIM to *in vivo* imaging of live zebrafish larvae and mouse brain (Turcotte et al., 2019). They imaged synapses with a resolution of 190 nm at ~10 frames per second and at a depth of ~25 µm. The key to SIM imaging in the brain was the implementation of wavefront correction with adaptive optics. The main challenge was the motion of brain structures at tens of Hertz frequency which was most probably owing to the pressure pulse of the beating heart. To compensate for this frame-to-frame motion, the authors speeded up the imaging, realigned images computationally, and averaged over several images (Figure 2). Post-processing such as averaging, however, is very critical when dynamic changes occur locally, for example, by morphological changes in dendritic spines. Therefore, it is of utmost importance to reduce motion as far as possible.

To image deeper in the tissue with SIM, the question is whether the illumination pattern can be generated with two-photon excitation. However, a direct application of a 2PE illumination pattern would require excessively high laser power. This is avoided by fast scanning of a focused two-photon excitation beam and by modulating it on/off so that a grating pattern is formed over time in the focal plane (Urban et al.,

2015); the pattern is rotated, shifted and the image detected by a camera as in the original one photon (1P) excitation SIM (Figure 1D). This technique was termed two-photon Super-resolution Patterned Excitation Reconstruction (2P-SuPER) microscopy and achieves a resolution of 119 nm with an acquisition of 3.5 images per second of a 21 μm large field of view (Urban et al., 2018). It was applied to imaging the living mouse cortex at a depth of 120 μm but reliable imaging of dendrites was hampered by brain motion and therefore image reconstruction was difficult.

Altogether, SIM has many advantages for live-cell imaging although the resolution improvement is restricted to a factor of two; it is relatively fast, and it works with standard fluorophores and low light intensities. Imaging *in vivo* is challenging mainly owing to brain motion; however, this might be suppressed by an optimized cranial window preparation as discussed below in the paragraph on obstacles when moving from imaging living tissue to live animal.

Image scanning microscopy with pixel reassignment

The most well-known and widespread technique to achieve optical sectioning is confocal microscopy. Its principle idea is to focus light on a spot and detect only the light coming from a small "confocal" region of this illumination spot. This is achieved by a pinhole in front of the detector, which rejects light coming from anywhere else than the focal spot (Figure 1B) (Pawley, 2006; Sheppard, 2021b). An image is acquired either by scanning the illumination and detected light beams over the sample or by moving the sample through the focal spot. Such a point-by-point illumination and detection is relatively slow; to speed up the imaging, illumination, and detection can be parallelized in a spinning disk confocal microscope by using a rotating array of pinholes and microlenses (Egger and Petráň, 1967; Pawley, 2006). Although the optical sectioning property is probably its main advantage, confocal microscopy also improves the resolution slightly over conventional imaging as its overall PSF is a product of the illumination PSF and the detection PSF. For infinitely small pinholes, the FWHM of the PSF is thus reduced by a factor of $\sim\sqrt{2}$, which comes at the expense of suppressing most of the light resulting in a bad signal-to-noise ratio. The light, which is rejected by the confocal pinhole, however, bears valuable information and can be used to improve the signal-to-noise ratio and resolution by a method termed pixel reassignment and/or image scanning microscopy (ISM) (Müller and Enderlein, 2010; Sheppard, 1987). Here, an array detector or a camera is used to detect the whole signal. As each detector pixel functions as a small pinhole, off-center pixels record shifted confocal images of similar resolution to the central pinhole but with lower intensity (Sheppard, 1987; Sheppard et al., 2013). The signal of each off-axis pixel is then reassigned to the coordinate from where it originated, which is about half of the distance of the detector pixel from the center (Figure 1E). The sum of the reassigned signal provides images with slightly improved resolution compared to confocal imaging; the main advantage, however, is the gain in peak signal (Sheppard et al., 2013). This comes, however, at the cost of a lower optical sectioning capability (Sheppard et al., 2013).

ISM was first implemented by Mueller and Enderlein in 2010 (Müller and Enderlein, 2010). The speed of this first implementation was relatively slow, limited by the acquisition speed of the camera detection. Thereafter, image acquisition was accelerated by multifocal illumination and detection (Schulz et al., 2013; York et al., 2012). Exchanging the digital pixel reassignment of the camera by performing optically reconstructions that decrease the emission spot before detection, increased the acquisition speed up to 100 Hz, a method termed instant SIM (York et al., 2013). The implementation of 2PE enabled imaging at depth of ~100 μm and frame rates of 1 Hz (Winter et al., 2014). This is shown, for example, by imaging the microtubule network in the developing lens of a zebrafish eye (Figure 3). With minor modifications 2PE ISM/instant SIM, was applied to imaging neuronal structures several hundred micrometer deep in brain slices (Koho et al., 2020). As these samples were fixed and cleared, it is difficult to transfer these result to *in vivo* imaging. Recently, ISM was used to live image the cone photoreceptor in the retina of the human eye (DuBose et al., 2019).

In summary, the speed of image recording is similar to confocal scanning microscopy and can be increased by parallelization, it inherits the confocal sectioning capability, albeit in slightly reduced form, and it does not require specific dyes. With the gain in the signal over confocal microscopy, ISM with pixel reassignment may be well suited for *in vivo* imaging.

Stimulated emission depletion microscopy

While the previously discussed SIM and ISM only offer a maximum of 2-fold resolution improvement, the resolution of STED microscopy is, in theory, unlimited. STED circumvents the diffraction limit by exploiting

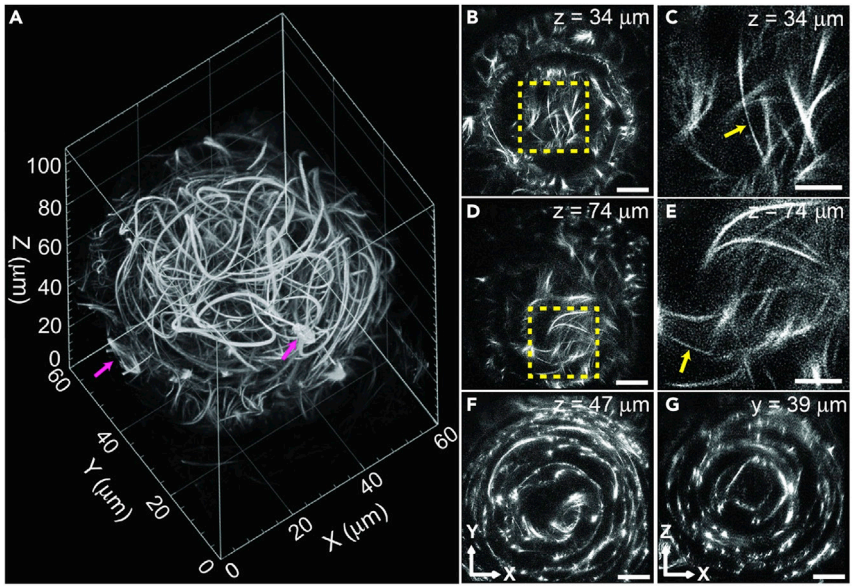

Figure 3. Two-photon excitation instant SIM of the EGFP-tagged microtubular network in a zebrafish eye

The 38–40 h old embryo is alive and microtubules are tagged with EGFP.

(A) Volume rendering of 110 µm depth in z. Dividing cells are marked by arrows (magenta).

(B, D, and F) X-Y image at indicated z-position. (C, E) Magnified view of the area marked in (B, D); arrows (yellow) mark thin microtubule of width <200 nm. (G) X-Z slice at indicated y-position showing a circular organization of the microtubular network. (A–G) Images are de-convolved. Scale bars: 10 µm (B, D, F, G); 5 µm (C, E). Adapted with permission from (Winter et al., 2014).

the fact that both states of a fluorescent molecule, the ground state, and the excited state, can be controlled by light. Thus, after on-switching or exciting the fluorescent molecule to an excited state, it can be depleted with light, a process termed stimulated emission depletion (Eggeling et al., 2015; Hell and Wichmann, 1994; Sahl et al., 2019). Such depletion, however, is only possible within a short time window before the emission of spontaneous fluorescence occurs. To achieve super-resolution, the depletion needs to be confined to the outer region of the excitation spot. For that purpose, the STED focal spot is shaped so that it features an intensity of zero in the center, for example by creating a donut-shaped intensity distribution (Figure 1F). Saturation of the depleting transition leads to an improvement in resolution, virtually breaking the diffraction barrier. With this technique, fluorescence is only emitted from a small central region size $\Delta r \approx \lambda / NA\sqrt{1 + I/I_{sat}}$ (Eggeling et al., 2015; Harke et al., 2008). Here, NA denotes the numerical aperture and I_{sat} a dye-specific value for the saturating laser intensity. Most importantly, by this formula, the spatial resolution of the microscope is tuned by the intensity I of the STED laser and scales with $\sim 1/\sqrt{I}$. In most cases STED microscopy is realized in a confocal spot-scanning arrangement and therefore takes over the sectioning capability of the pinhole detection (Figure 1B), which renders STED applicable in tissue. In principle, most fluorescent dyes can be employed for STED by tuning the excitation and depletion wavelengths to the spectral properties of the fluorescent dye; this includes for live-cell imaging fluorescent proteins such as EGFP (Willig et al., 2006), EYFP (Nagerl et al., 2008), organic dyes, e.g. coupled via SNAP-tags (Bottanelli et al., 2016; Hein et al., 2010), silicon-rhodamine probes for actin or tubulin (Lukinavičius et al., 2014) or red-emitting fluorescent proteins (Wegner et al., 2017).

It is often criticized that the laser intensities in STED microscopy are high and therefore detrimental for living cells or *in vivo* imaging. Indeed, the STED power for *in vivo* imaging is in the range of tens of mW in comparison to an excitation of a few µW (Wegner et al., 2022; Willig et al., 2014). The depletion intensity is, therefore, ~1000 times higher than that of the excitation laser. However, there are fundamental differences between excitation and depletion in terms of their effects on phototoxicity. A major part of phototoxicity is caused by the generation of long-living metastable dark states which then interact with molecular oxygen to form reactive oxygen species (ROS) that is cytotoxic for the cell (Eggeling et al., 2015; Laissue et al., 2017). In this process, the fluorescent molecule loses its ability to fluoresce and thus bleaches. Such dark states are only created by the crossing of an electron from an excited state and naturally happens

at a very low probability at each excitation. Therefore, the longer or the more often a molecule resides in an excited state, the more likely it is converted to a dark state. The STED depletion causes the molecule to be de-excited and therefore it is not thought to be a major source of ROS formation. Moreover, the STED light is always ~100 nm red-shifted compared to the excitation wavelength, which is less phototoxic. However, photobleaching, indeed, poses a limit for time-lapse STED imaging for several reasons. Decreasing the effective focal volume by STED requires much smaller pixel sizes and therefore each molecule is excited more often than in conventional imaging; for this reason, the effective photobleaching is often higher with super-resolution. To reduce photodamage, the ROS can be trapped by a ROS-scavenging buffer (*in vitro* only) (Kilian et al., 2018), or reduced through triplet-state relaxation; either by reducing the repetition rate of excitation/depletion (Donnert et al., 2006) or fast scanning (Kilian et al., 2018). Moreover, the phototoxicity can be reduced by intelligent light exposure schemes, which switch on the light only when needed (Staudt et al., 2011) or adapt it dynamically (Heine et al., 2017).

In 2012 we used STED microscopy for the first time to super-resolve the processes of a neuronal cell expressing EGFP with a resolution <70 nm in the mouse cortex (Berning et al., 2012). Moreover, we imaged filamentous actin in dendrites with 43–70 nm resolution down to a depth of 40 μm simply by compensating spherical aberrations with the correction collar of the objective lens (Willig et al., 2014). Recently, we extended the observation period and chronically monitored dendritic spines for up to one month with a resolution of <100 nm (Figure 4A) (Steffens et al., 2021). Moreover, we extended *in vivo* imaging to triple-label STED microscopy, the quasi-simultaneous imaging of three different protein structures by exploiting reversibly switchable fluorescent proteins (RSFP) (Figure 4B) (Willig et al., 2021). For all these studies, we used green/yellow emitting fluorescent proteins with a blue excitation and 595 nm stimulated emission depletion mainly because of their superior brightness. Imaging with red light is, in principle, less phototoxic (Kilian et al., 2018) but *in vivo* STED imaging of filamentous actin (Wegner et al., 2017) was relatively dark with the red-emitting fluorescent protein mNeptune2, owing to its low quantum yield (Lin et al., 2009).

This selection shows that *in vivo* super-resolution with STED microscopy has matured to become a valuable tool for nanoscale imaging in living mice. A drawback of this method could be the relatively slow scanning speed. With a typical pixel dwell time of 5 μs (Steffens et al., 2021), it takes ~5 s to capture an image of 30 × 30 μm size. This is much slower than the 10 frames per second reached *in vivo* with SIM. However, as STED is a spot scanning technique, the frame rate is much higher for smaller images; for example, 3 × 3 μm image sizes are acquired 100 times faster within ~0.05 s. Moreover, dynamic changes in structures, such as of living cells or *in vivo*, may be more easily recorded by a scanning technique. Motion slower than a few line scans is not visible in a scanned image, but each movement within the capturing of a single camera frame will blur the structure and complicate reconstruction as required, for instance, for SIM.

Two-photon excitation stimulated emission depletion microscopy

Another method to achieve optical sectioning is using non-linear excitation. Instead of a single photon, two photons of roughly double the wavelength and thus half the photon energy can combine their energy in order to excite a fluorescent molecule when they are both absorbed within a short time interval. This process requires high photon densities, which are only achieved in a spatially confined, perifocal region. Therefore, all fluorescence photons originate from near the focus and can be counted without spatial filtering by a confocal pinhole (Figure 1C). This spatial confinement is maintained even in high scattering tissue and is, therefore, particularly advantageous for deep tissue imaging (Helmchen and Denk, 2005). A further advantage is that the use of a longer, far-red wavelength helps to reduce the overall photodamage. As such, 2PE microscopy is state-of-the-art to observe sub-cellular structures *in vivo* (Helmchen and Denk, 2005; Holtmaat et al., 2009). To increase the spatial resolution, stimulated emission depletion can be performed as well after 2PE in the same way as described above for one photon excitation (1PE) (Figure 1G) (Moneron and Hell, 2009). Its applicability for tissue imaging was first shown in acute brain slices (Bethge et al., 2013). After implanting a window over the hippocampus deep within the brain, 2PE STED microscopy revealed a high turnover of dendritic spines *in vivo* within 4 days (Figure 4C) (Pfeiffer et al., 2018). By combining adaptive optics and red-emitting organic dyes, the penetration depth was improved with this method to 76 μm in the living mouse cortex (Velasco et al., 2021).

The size of the 2PE area is slightly larger than that of the 1PE. The doubling of the wavelength for 2PE doubles the size of the excitation illumination and the quadratic dependence of the emission on the excitation

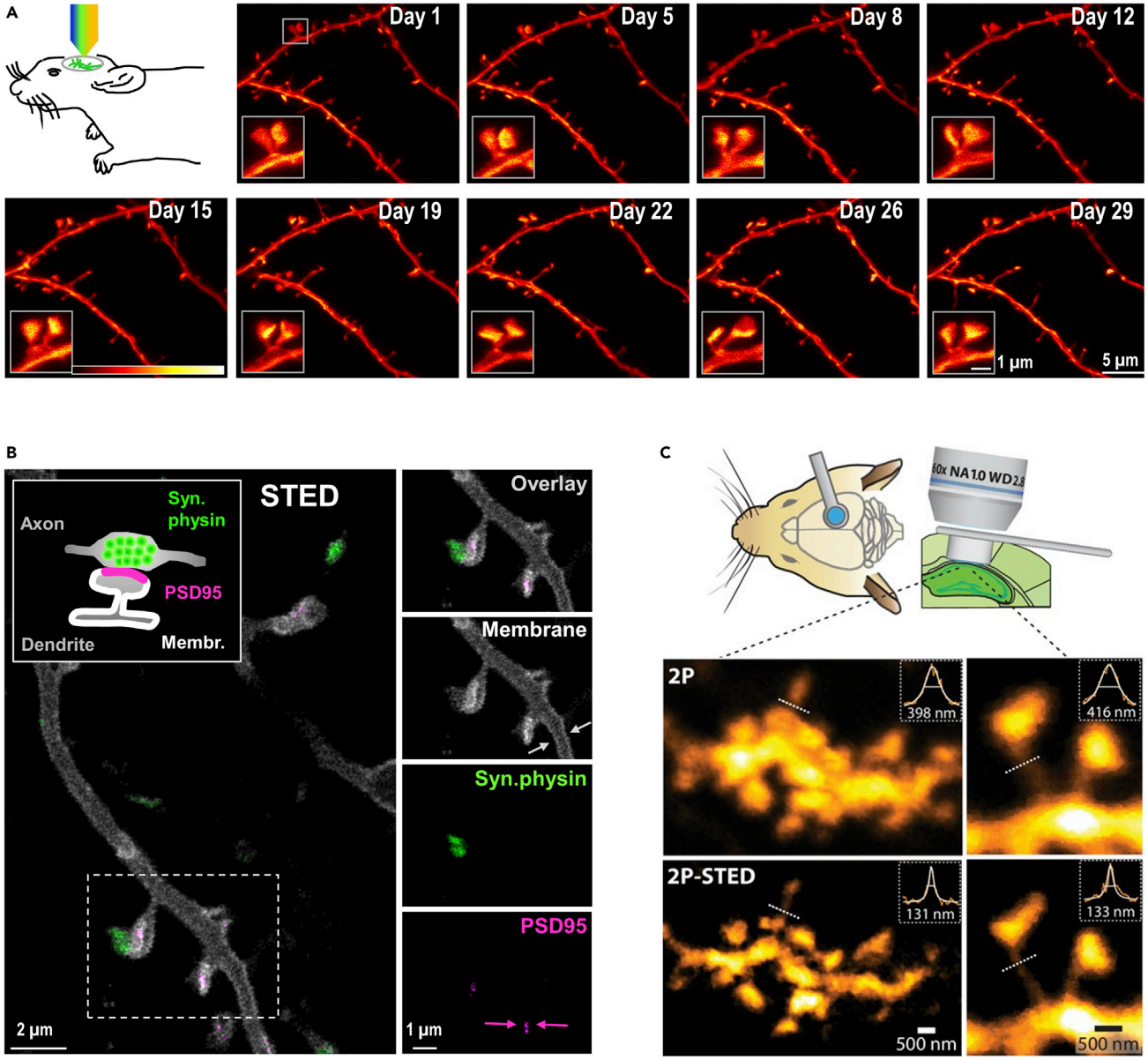

Figure 4. State-of-the-art *in vivo* STED microscopy

(A) Chronic STED imaging of EGFP expressing dendritic stretches in layer 1 of the motor cortex for up to one month.

(B) Triple-label *in vivo* STED microscopy of the pre- and postsynaptic nanoorganizations in the mouse visual cortex utilizing EGFP (Synaptophysin, green), Citrine (PSD95.FingR, magenta), and the RSFP rsEGP2 (Membrane, white).

(C) Chronic two-photon excitation STED (2P-STED) microscopy and corresponding two-photon image (2P) of dendritic spines in the hippocampus. Adapted from (Steffens et al., 2021) (A), (Willig et al., 2021) (B) and (Pfeiffer et al., 2018) (C).

intensity reduces the effective focal excitation by $\sqrt{2}$. Hence, the resolution of a 2PE microscope is roughly $\sqrt{2}$ lower than that of the corresponding 1PE. However, the resolution for large STED intensities does not depend on whether STED is combined with 1PE or 2PE as the achievable resolution mostly depends on the depletion laser intensity as discussed above. As stimulated depletion is inherently a one-photon process, the use of 2PE in STED does not help to improve the penetration depth. The benefits of 2PE for STED are rather its potentially lower phototoxicity, especially compared to 1PE with blue light and superior sectioning capability for densely labeled tissue. The spectral separation of different labels, however, is more difficult for 2PE; the discrimination of the labels solely by spectrally separated detection requires spectral unmixing (Pfeiffer et al., 2018).

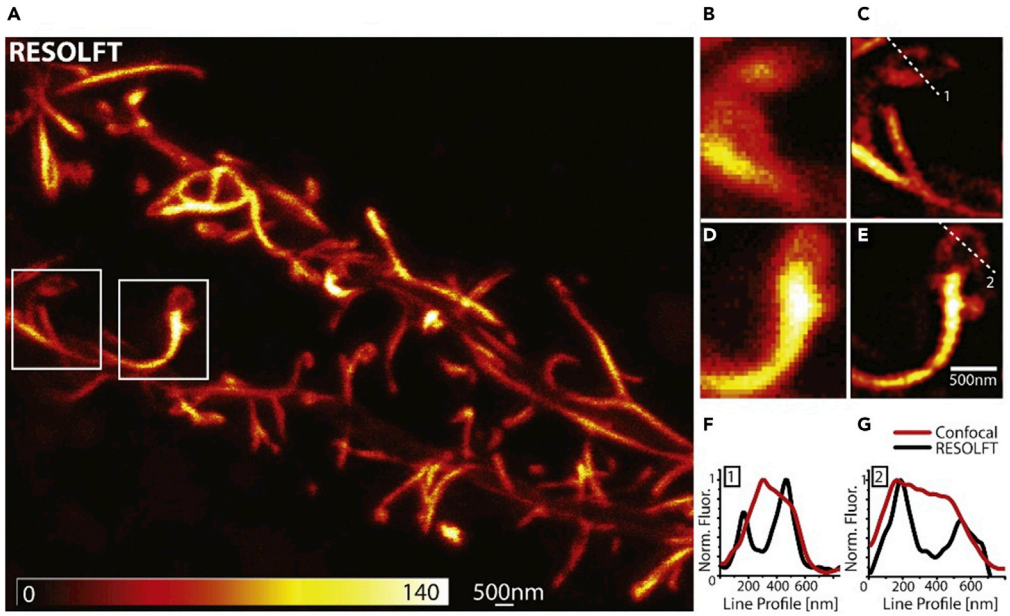

Figure 5. RESOLFT microscopy of live organotypic hippocampal brain slice

(A) Dendrites expressing the actin marker Lifeact-Dronpa-M159T ~38 μm deep in the tissue.

(B–D) Magnifications of the boxed area in (A) show that the actin is super-resolved by RESOLFT (C, E) but not in the corresponding confocal image (B, D).

(F and G) Line profiles along the lines in (C, D) indicate the superior resolution of RESOLFT microscopy. Reprinted from (Testa et al., 2012), with permission from Elsevier.

The key to the improvement of the depth penetration of STED microscopy, independently whether it is combined with 1PE or 2PE, will be the application of adaptive optics such as shown in (Velasco et al., 2021). This is particularly important when performing STED in 3D, as the quality of the intensity minimum of the 3D STED PSF is more susceptible to optical aberrations than the intensity minimum of the STED donut that is typically used for 2D resolution enhancement (Velasco et al., 2021).

Reversible saturable optical fluorescence transition microscopy

The conception of STED is generalized by the idea that any saturable transition between a bright and a dark state, which can be driven by light can be used to circumvent the diffraction limit, a concept termed RESOLFT nanoscopy (Hell et al., 2003, 2004). Such an on-/off-state is achievable, for example, with reversibly switchable fluorescent proteins (RSFP). By a change in their molecular conformation, RSFPs can be switched from a fluorescent on-state to a long-living, dark off-state. The main benefit of using states with long lifetime is that it reduces the light intensities required for switching by orders of magnitude over the depletion intensity in STED microscopy. This advantage is particularly valuable for live-cell or *in vivo* imaging. The first experimental proof of super-resolution with RSFPs was performed with asFP595 in 2005 (Hofmann et al., 2005). With the development of faster switching RSFPs, imaging of living cells (Grotjohann et al., 2012) or brain slices (Testa et al., 2012) became possible (Figure 5). Live-cell imaging with the fast switching rsEGFP2 is performed with off-switching blue light at 10 kW/cm^2, which is about 1000 times less than what is used for STED imaging of EGFP of EYFP (~20 mW STED power, corresponding to ~10 MW/cm^2 (Steffens et al., 2021; Willig et al., 2014)). The long lifetime of the dark state, however, is accompanied by relatively slow switching kinetics. Thus, the pixel dwell time for RESOLFT microscopy is ~100 times longer than that for STED microscopy, which puts the photon budget between STED and RESOLFT into perspective. The initial RESOLFT implementations were based on a scanning scheme and confocal detection similar to STED microscopy (Figure 1H), which can be readily used for tissue imaging (Figure 5). Thereafter, the imaging speed was significantly increased to <1 s per frame by parallelizing the switching in the widefield; two incoherently superimposed orthogonal standing waves produce a pattern with thousands of intensity zeros for local off-switching (Chmyrov et al., 2013). Implementing a multi-foci pattern for on-switching and readout instead of the uniform illumination used by Chmyrov et al. improved the optical sectioning capability in an approach termed Molecular Nanoscale Live Imaging

with Sectioning Ability (MoNaLISA) (Masullo et al., 2018). Moreover, this technique improved the photon output, which extended time-lapse imaging to 40-50 frames at consistent high frame rate of ~1 Hz. As sectioning is achieved by focused activation of relatively short UV light of 405 nm and focused blue excitation, MoNaLISA improves the optical sectioning over that of a confocal detection (Masullo et al., 2018). However, imaging deep in tissue has not yet been performed, and future experiments will reveal whether cross-talk between the parallelized foci will hinder imaging in tissue and thus whether imaging *in vivo* will be practical.

OBSTACLES WHEN MOVING FROM IMAGING LIVING TISSUE TO LIVE ANIMAL

Imaging in a living organism imposes several challenges beyond optical considerations. Although tissue-induced aberrations and scattering of the light *in vivo* is similar to imaging of living tissue *in vitro*, several factors hamper imaging in the living mouse brain. First, intrinsic factors such as heartbeat or pressure pulse can easily cause motion artifacts. The cortex is interspersed with a dense network of capillaries and arteries; the diffusion of blood cells through these blood vessels can cause a movement of the surrounding brain tissue with the frequency of the beating heart, which is ~300 beats per minute for the anesthetized mouse. Similarly, the spontaneous breathing of the mouse might impose periodic movement. Such motion is primarily suppressed by a rigid mounting of the skull by gluing a metal bar to the skull bone. In addition, we believe that great attention must be paid to the way in which the coverslip is implanted. It is of crucial importance that the coverslip is very close to the brain surface. At distances >5 μm between the window and the brain surface, we usually experienced motion artifacts. Such distances could be reduced by extracting the cerebrospinal fluid through a drainage tube that was implanted below the window. For details of the preparation see (Steffens et al., 2020). Beyond these disturbances owing to vital functions, there are several extrinsic factors that impede super-resolution imaging *in vivo*. As the anesthesia goes along with a reduction in the body temperature, it is required to heat the mouse. The heating usually needs to be adapted with the depth of the anesthesia and is, therefore, not necessarily constant. Care needs to be taken to implement such heating without causing a thermal drift of the super-resolution microscope. According to our experience, a critical parameter is also the type of glue used for mounting the coverslip and the skull. Especially for the coverslip, it is important to use a resin cement with low polymerization shrinkage as such a shrinkage easily introduces a bending of the coverslip, which in turn induces additional aberrations on the wavefront of the light beams. Moreover, a slowly curing cement may lead to drift when imaging directly after the window implantation owing to persistent shrinkage. We solved most of these problems by using a dental resin cement with polymethyl methacrylate being the main component (Super-Bond C&B, Sun Medical Co. LTD, Japan) (Steffens et al., 2020).

These considerations are critical for all *in vivo* super-resolution techniques and are not specific to STED microscopy. Owing to the increased resolution and typically slower scanning speed or camera detection, all super-resolution techniques are much more affected by motion artifacts than the traditionally used 2PE microscopy.

HURDLES OF TAGGING STRUCTURES *IN VIVO*

A very common and frequently used mouse line for *in vivo* imaging of dendritic spines by 2PE microscopy is the thy1-EGFP or EYFP mouse, a transgenic line expressing the fluorescent protein in the cytosol of projection neurons under the control of neuron-specific elements from the thy1 gene (Feng et al., 2000). With the help of this line, many *in vivo* methods were implemented, such as chronic window implantation (Holtmaat et al., 2009), and proof-of-principle of super-resolution *in vivo* methods such as STED microscopy (Berning et al., 2012; Pfeiffer et al., 2018; Steffens et al., 2021) or SIM (Turcotte et al., 2019). However, with a super-resolution of <100 nm, the observation of smaller, sub-cellular structures and nanoorganizations is within reach. Therefore, there is a quest for a reliable *in vivo* labeling of, for instance, synaptic proteins, receptors, and so forth. Nonetheless, not all live cell labeling approaches are applicable *in vivo* or in tissue sections. For example, SiR-actin, a fluorogenic probe labeling actin is excellent and widely used to reveal the ring structure of actin with STED microscopy in living cells (Lukinavičius et al., 2014). However, the injection of such a probe into the brain would result in a highly dense labeling as all brain cells contain actin. Thus, *in vivo* labeling mostly requires that a subset of cells can be addressed – a demand achievable with genetic tagging. Genetic tagging can be roughly divided into two categories: The expression of a fusion protein of the protein of interest with, for instance, a fluorescent protein or exogenous probes that bind the endogenous protein of interest at high affinity. Fusion proteins can be conveniently expressed *in vivo* via viral vector techniques such as recombinant adeno-associated viral particles or lentiviruses. For synaptic proteins, however, such overexpressions often affect the synaptic function as, for example, shown

for overexpression of PSD95-GFP (El-Husseini et al., 2000). Alternatively, the expression of fusion proteins as a transgenic knock-in maintains endogenous protein level and function, for example, PSD95-GFP (Broadhead et al., 2016) or VGlut1-Venus mice (Herzog et al., 2011), but it is very time-consuming to establish such mouse lines. Substituting the fluorescent protein with an enzymatic self-labeling HaloTag allows the use of more photo-stable organic dyes. The drawback of this method for *in vivo* applications is that the substrate with the organic dye is not yet penetrating the blood-brain barrier and needs to be injected into the cortex before imaging (Masch et al., 2018).

In contrast, intracellular expression of proteins or peptides that bind post-translationally to specific endogenous proteins is potentially less susceptible to affecting protein function but also have some pitfalls. Such intrabodies can be genetically fused with fluorescent proteins and expressed in cells *in vivo*. Many intrabodies are antibody fragments of heavy-chain only antibodies of camelids termed nanobodies. However, only nanobodies not relying on the formation of disulfide bonds can be expressed in living cells (for a detailed review (Wagner and Rothbauer, 2020)). The fusions of nanobodies with fluorescent proteins are termed chromobodies. Meanwhile, a large range of chromobodies exist, targeting the cytoskeleton, nuclear components (Traenkle and Rothbauer, 2017), or neuronal protein such as, for instance, Homer1 and Gephyrin (Dong et al., 2019). Another approach to create intrabodies is relying on antibody-like proteins based on a fibronectin scaffold termed FingR (fibronectin intrabodies generated by mRNA display) (Gross et al., 2013). Available FingRs target PSD95, Gephyrin (Gross et al., 2013), and CamKII (Cook et al., 2019). An alternative intrabody targeting F-actin is the small peptide Lifeact, derived from the yeast F-actin-binding protein Abp140 (Riedl et al., 2008).

A common challenge for all exogenous labels and overexpressions is that the number of expressed fusion proteins needs to match the number of free binding sites as close as possible. Too high expression results in high cytosolic background and too low expression in low fluorescent signal. An elegant approach to adjust the intrabody expression level was applied to the FingR constructs. A negative feedback regulation consisting of a DNA-binding zinc finger domain and the transcriptional repressor domain KRAB-A inhibits the transcription of the FingR when all binding sites are occupied (Gross et al., 2013). Recently, other approaches on this line utilize a light activation of nanobodies (Yu et al., 2019) or activation and deactivation with small molecules (Farrants et al., 2020).

Although the search for intrabodies is very elaborate and the number of reliable markers is still limited, their genetic encodability and tagging of endogenous proteins are ideal for super-resolution *in vivo* imaging. Nevertheless, it is important to keep an eye on whether the new intrabodies interfere with the function of the target, as was observed for intrabodies labeling F-actin at high expression levels, for example (Courtemanche et al., 2016; Kumari et al., 2020; Wegner et al., 2017). An approach that largely avoids such negative influences is inverse labeling of brain tissue, known as super-resolution shadow imaging (SUSHI) (Tønnesen et al., 2018), although this is limited to observing the anatomy of brain cells.

INSIGHTS GAINED SO FAR WITH *IN VIVO* SUPER-RESOLUTION

So far, all studies utilizing *in vivo* super-resolution that are beyond a proof-of-concept have focused on neuronal plasticity and proteins of synapses, the connection formed between two neurons. Although synapse and spine plasticity has been studied for more than two decades with 2PE microscopy, many questions remain unanswered owing to its diffraction-limited resolution. From 2PE *in vivo* studies it is known that synapses undergo extensive elimination and formation even under baseline conditions (De Paola et al., 2006; Holtmaat et al., 2005). Synaptic connections, however, are not binary on/off units but undergo changes in synaptic strength by a remodeling within the pre- and postsynaptic elements owing to activity. There is an ongoing debate about whether and how much such synaptic changes contribute to the storage and retrieval of memory (Langille and Brown, 2018). Recently, it became evident that pre- and postsynaptic proteins such as receptors or scaffolding proteins form a patterned distribution, which is changed by activity and might influence the synaptic strength by rearrangement or concerted alignment between pre- and postsynapse (Compans et al., 2016; Carvalhais et al., 2021; Tang et al., 2016). The study of such a nanoplasticity is beyond the capability of classical, diffraction-limited light microscopy. Super-resolution techniques now open the way to investigate the plasticity of such nanostructures in living cells and eventually in the intact mouse.

With our advanced longitudinal *in vivo* STED microscopy of dendritic spines (Figure 4A), we found that spines that persist for weeks show substantial fluctuations in head size, neck length, and neck width within

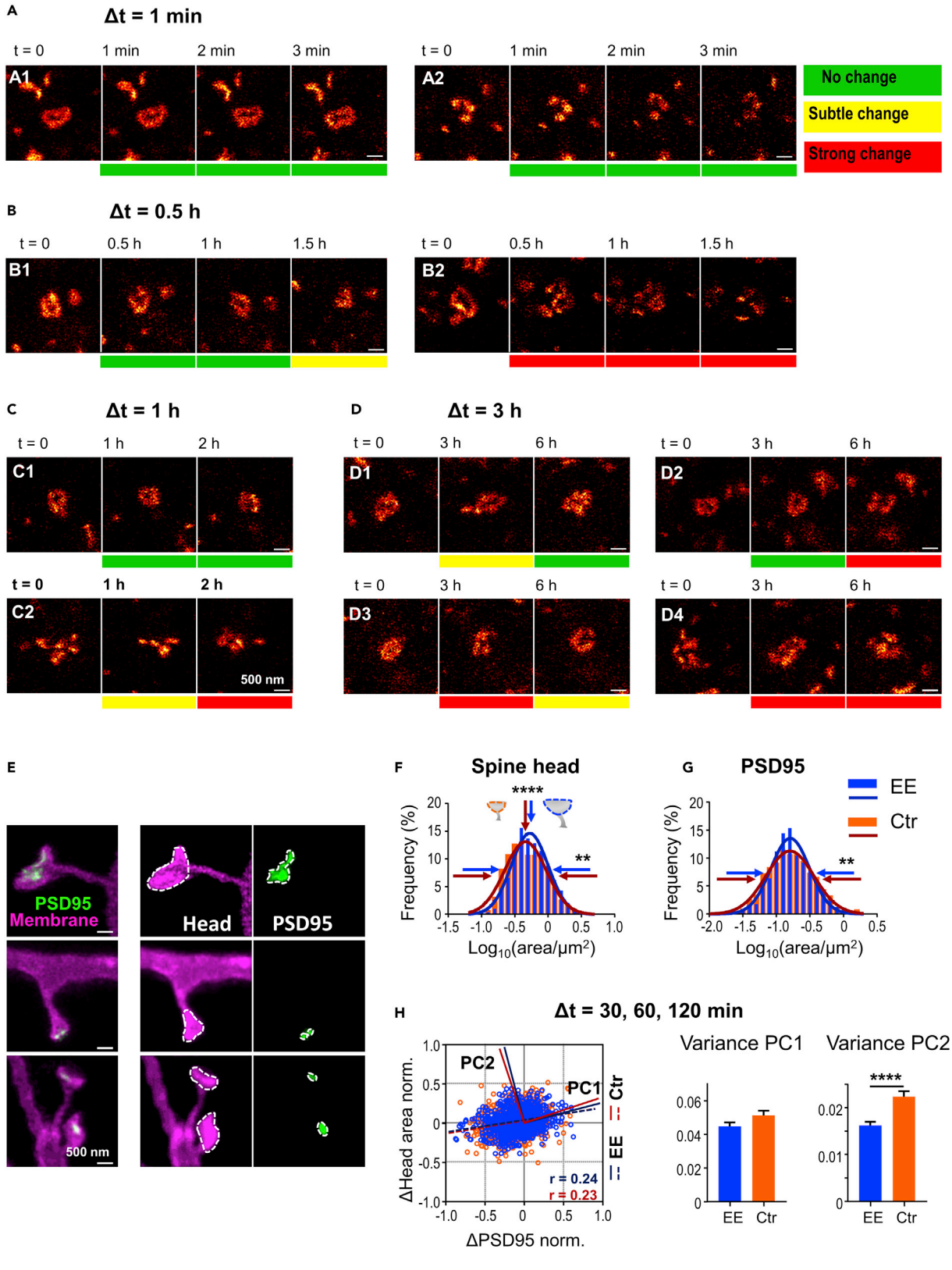
A
Δt = 1 min
t = 0
1 min
2 min
3 min
A1
A2
No change
Subtle change
Strong change
B
Δt = 0.5 h
t = 0
0.5 h
1 h
1.5 h
B1
B2
C
Δt = 1 h
t = 0
1 h
2 h
C1
C2
500 nm
D
Δt = 3 h
t = 0
3 h
6 h
D1
D2
D3
D4
E
PSD95
Membrane
Head
PSD95
500 nm
F
Spine head
****
**
Frequency (%)
Log10(area/μm2)
G
PSD95
EE
Ctr
**
Frequency (%)
Log10(area/μm2)
H
Δt = 30, 60, 120 min
PC2
PC1
Ctr
EE
r = 0.24
r = 0.23
ΔHead area norm.
ΔPSD95 norm.
Variance PC1
Variance PC2
****
EE
Ctr
EE
Ctr

Figure 6. *In vivo* STED microscopy of synaptic nanostructure and its nanoplasticity

(A–D) Adult knock-in mouse expressing EGFP fused to the endogenous PSD95 protein; imaged in the visual cortex at baseline. The nanoorganization of large PSD95 assemblies is very diverse in structure and dynamic; while the nanostructure is stable over minutes it changes substantially after 1 h.

(E–H) Changes in synaptic nanopattern and plasticity after environmental enrichment (EE) compared to mice housed in standard cages (Ctr). Endogenous PSD95 is labeled with the intrabody FingR.PSD95 fused to Citrine and the dendritic membrane with a myristoylation site fused to EGFP (E). Environmental enrichment, which is associated with enhanced activity increases the average spine head size (F) while the distribution of sizes of spine heads and PSD95 assemblies is less variable (F, G).

(H) Normalized changes in spine head and PSD95 area after Δt = 30, 60, and 120 min correlate only mildly (left); Pearson's correlation coefficient r. Changes in size are smaller for EE-housed mice (right); principle components (PC) of principal component analysis. Adapted from (Wegner et al., 2018) (A–D) and (Wegner et al., 2022) (E–H).

days (Steffens et al., 2021). These parameters changed largely uncorrelated indicating independent drivers of spine remodeling. *In vivo* STED microscopy also revealed a high turnover of dendritic spines in the hippocampus (Figure 4C) (Pfeiffer et al., 2018). In the synapse, we found extensive volatility of PSD95, a postsynaptic scaffolding protein (Figures 6A–6D). Recent evidence suggests that PSD95 is an important signaling platform anchoring neurotransmitter receptors, ion channels, and the actin cytoskeleton and thus contributes to changes in synaptic strength (Herring and Nicoll, 2016). With *in vivo* STED microscopy, we have shown that PSD95 is often organized in distinct clusters or assembled in a nanostructure comprising ring-like, horse-shoe, or more complex shapes. This nanopattern is stable within minutes but highly plastic within hours (Wegner et al., 2018). Although these studies were performed at baseline, i.e. without a stimulation, in the anesthetized mouse cortex we have also studied synaptic plasticity after enhanced activity (Figures 6E–6H). We found differences in size, nanoorganization and structural dynamics of spine heads and PSD95 in mice reared in an enriched environment, providing multi-sensory stimulation, cognitive activity, social interactions, and physical exercise (Wegner et al., 2022).

PERSPECTIVE

The applications summarized above show that *in vivo* super-resolution is able to play a vital role in brain research, for example in deciphering the functional role of synaptic nanopatterns. The major limitation of *in vivo* super-resolution to date is certainly the limited penetration depth, which is a fundamental limitation for all light microscopy techniques. Biological tissue is a heterogeneous mixture of proteins, protein complexes, lipids, and aqueous components. Variations in refractive indices of these constituents refract the penetrating light and cause aberrations that distort the PSF. Super-resolution microscopes are very sensitive to the smallest distortions as they lead to a degradation of the resolving power and not just to a loss of signal. In recent years adaptive optics has become a valuable tool to correct such aberrations and improve imaging quality deep in living specimen. Its basic idea is to compensate for the aberrations by adding an opposite amount of the distortion to the wavefront before entering the tissue. This is achieved by wavefront shaping devices such as deformable mirrors or spatial light modulators (Booth, 2014; Wang and Zhang, 2021) and was applied to improve the penetration depth of super-resolution *in vivo* microscopy (Turcotte et al., 2019; Velasco et al., 2021). However, a problem with adaptive optics is certainly that it is relatively difficult to apply. Although it is relatively straight forward to incorporate a wavefront shaping device into the optical path, it is challenging to correct the wavefront as accurately as required for super-resolution microscopy. For a review of the various sensing and correction schemes see (Booth, 2014).

With increasing tissue depth, the penetrating light is additionally distorted by scattering, which sets in at ~100 μm in brain tissue (Helmchen and Denk, 2005). This value is wavelength dependent; scattering increases strongly for light below 500 nm and decreases slowly for longer wavelengths (Jacques, 2013). For this reason, the penetration depth of all optical techniques is better in the red wavelength regime. In 2PE microscopy, mainly ballistic (non-scattered) photons contribute to the fluorescence signal owing to the non-linear excitation, so that scattering mainly leads to a degradation of the signal intensity. For super-resolution microscopy, however, scattering might impose a fundamental limit. For example, in STED and RESOLFT microscopy, switching off is a linear process; thus scattered photons of the donut beam into the intensity minimum would degrade the fluorescence signal significantly. It has long been considered impossible to correct the wavefront for such scattering events. However, the work of Vellekoop and Mosk proved that multiply scattered light can be controlled by complex wavefront shaping (Vellekoop and Mosk, 2007). This technique compensates also higher order wavefront distortions than traditional adaptive optics by utilizing wavefront modulators with a large number of pixels and advanced control routines (May et al., 2021; Papadopoulos et al., 2017; Park et al., 2015; Pozzi et al., 2020; Tang et al., 2012). Most impressively, such wavefront shaping was used to image microglia and neurons through the intact skull of

an adult mouse with 2PE (Park et al., 2015). The future will show whether such a complex scattering correction could also improve the depth penetration of super-resolution.

ACKNOWLEDGMENTS

I acknowledge Dr. Jan Keller-Findeisen, Dr. Heinz Steffens, and Jaydev Jethwa, Max Planck Institute for Multidisciplinary Sciences, for their critical reading.

AUTHOR CONTRIBUTIONS

The article was written and revised by KIW.

DECLARATION OF INTERESTS

The author declares no competing interests.

REFERENCES

Berning, S., Willig, K.I., Steffens, H., Dibaj, P., and Hell, S.W. (2012). Nanoscopy in a living mouse brain. Science *335*, 551. https://doi.org/10.1126/science.1215369.

Bethge, P., Chéreau, R., Avignone, E., Marsicano, G., and Nägerl, U.V. (2013). Two-photon excitation STED microscopy in two colors in acute brain slices. Biophys. J. *104*, 778–785. https://doi.org/10.1016/j.bpj.2012.12.054.

Booth, M.J. (2014). Adaptive optical microscopy: the ongoing quest for a perfect image. Light Sci. Appl. *3*, e165–7. https://doi.org/10.1038/lsa.2014.46.

Bottanelli, F., Kromann, E.B., Allgeyer, E.S., Erdmann, R.S., Wood Baguley, S., Sirinakis, G., Schepartz, A., Baddeley, D., Toomre, D.K., Rothman, J.E., and Bewersdorf, J. (2016). Two-colour live-cell nanoscale imaging of intracellular targets. Nat. Commun. *7*, 10778–10785. https://doi.org/10.1038/ncomms10778.

Broadhead, M.J., Horrocks, M.H., Zhu, F., Muresan, L., Benavides-Piccione, R., DeFelipe, J., Fricker, D., Kopanitsa, M.V., Duncan, R.R., Klenerman, D., et al. (2016). PSD95 nanoclusters are postsynaptic building blocks in hippocampus circuits. Sci. Rep. *6*, 24626. https://doi.org/10.1038/srep24626.

Carvalhais, L.G., Martinho, V.C., Ferreiro, E., and Pinheiro, P.S. (2021). Unraveling the nanoscopic organization and function of central mammalian presynapses with super-resolution microscopy. Front. Neurosci. *14*, 578409. https://doi.org/10.3389/fnins.2020.578409.

Chmyrov, A., Keller, J., Grotjohann, T., Ratz, M., D'Este, E., Jakobs, S., Eggeling, C., and Hell, S.W. (2013). Nanoscopy with more than 100, 000 "doughnuts. Nat. Methods *10*, 737–740. https://doi.org/10.1038/nmeth.2556.

Compans, B., Choquet, D., and Hosy, E. (2016). Review on the role of AMPA receptor nano-organization and dynamic in the properties of synaptic transmission. Neurophotonics *3*, 041811. https://doi.org/10.1117/1.NPh.3.4.041811.

Cook, S.G., Goodell, D.J., Restrepo, S., Arnold, D.B., and Bayer, K.U. (2019). Simultaneous live imaging of multiple endogenous proteins reveals a mechanism for alzheimer's-related plasticity impairment. Cell Rep. *27*, 658–665.e4. https://doi.org/10.1016/j.celrep.2019.03.041.

Courtemanche, N., Pollard, T.D., and Chen, Q. (2016). Avoiding artefacts when counting polymerized actin in live cells with LifeAct fused to fluorescent proteins. Nat. Cell Biol. *18*, 676–683. https://doi.org/10.1038/ncb3351.

De Paola, V., Holtmaat, A., Knott, G., Song, S., Wilbrecht, L., Caroni, P., and Svoboda, K. (2006). Cell type-specific structural plasticity of axonal branches and boutons in the adult neocortex. Neuron *49*, 861–875. https://doi.org/10.1016/j.neuron.2006.02.017.

Denk, W., Strickler, J.H., and Webb, W.W. (1990). Two-photon laser scanning fluorescence microscopy. Science *248*, 73–76. https://doi.org/10.1126/science.2321027.

Dong, J.X., Lee, Y., Kirmiz, M., Palacio, S., Dumitras, C., Moreno, C.M., Sando, R., Santana, L.F., Südhof, T.C., Gong, B., et al. (2019). A toolbox of nanobodies developed and validated for use as intrabodies and nanoscale immunolabels in mammalian brain neurons. Elife *8*, e48750–25. https://doi.org/10.7554/eLife.48750.

Donnert, G., Keller, J., Medda, R., Andrei, M.A., Rizzoli, S.O., Lührmann, R., Jahn, R., Eggeling, C., and Hell, S.W. (2006). Macromolecular-scale resolution in biological fluorescence microscopy. Proc. Natl. Acad. Sci. USA *103*, 11440–11445. https://doi.org/10.1073/pnas.0604965103.

DuBose, T.B., LaRocca, F., Farsiu, S., and Izatt, J.A. (2019). Super-resolution retinal imaging using optically reassigned scanning laser ophthalmoscopy. Nat. Photonics *13*, 257–262. https://doi.org/10.1038/s41566-019-0369-7.

Eggeling, C., Willig, K.I., Sahl, S.J., and Hell, S.W. (2015). Lens-based fluorescence nanoscopy. Q. Rev. Biophys. *48*, 178–243. https://doi.org/10.1017/s0033583514000146.

Egger, M.D., and Petrăn, M. (1967). New reflected-light microscope for viewing unstained brain and ganglion cells. Science *157*, 305–307. https://doi.org/10.1126/science.157.3786.305.

El-Husseini, A.E.-D., Schnell, E., Chetkovich, D.M., Nicoll, R.A., and Bredt, D.S. (2000). PSD-95 involvement in maturation of excitatory synapses. Science *290*, 1364–1368. https://doi.org/10.1126/science.290.5495.1364.

Farrants, H., Tarnawski, M., Müller, T.G., Otsuka, S., Hiblot, J., Koch, B., Kueblbeck, M., Kräusslich, H.G., Ellenberg, J., and Johnsson, K. (2020). Chemogenetic control of nanobodies. Nat. Methods *17*, 279–282. https://doi.org/10.1038/s41592-020-0746-7.

Feng, G., Mellor, R.H., Bernstein, M., Keller-Peck, C., Nguyen, Q.T., Wallace, M., Nerbonne, J.M., Lichtman, J.W., and Sanes, J.R. (2000). Imaging neuronal subsets in transgenic mice expressing multiple spectral variants of GFP. Neuron *28*, 41–51. https://doi.org/10.1016/S0896-6273(00)00084-2.

Gross, G.G., Junge, J.A., Mora, R.J., Kwon, H.B., Olson, C.A., Takahashi, T.T., Liman, E.R., Ellis-Davies, G.C.R., McGee, A.W., Sabatini, B.L., et al. (2013). Recombinant probes for visualizing endogenous synaptic proteins in living neurons. Neuron *78*, 971–985. https://doi.org/10.1016/j.neuron.2013.04.017.

Grotjohann, T., Testa, I., Reuss, M., Brakemann, T., Eggeling, C., Hell, S.W., and Jakobs, S. (2012). rsEGFP2 enables fast RESOLFT nanoscopy of living cells. Elife *1*. e00248–14. https://doi.org/10.7554/eLife.00248.

Gustafsson, M.G.L. (2005). Nonlinear structured-illumination microscopy: wide-field fluorescence imaging with theoretically unlimited resolution. Proc. Natl. Acad. Sci. USA *102*, 13081–13086. https://doi.org/10.1073/pnas.0406877102.

Gustafsson, M.G. (2000). Surpassing the lateral resolution limit by a factor of two using structured illumination microscopy. J. Microsc. *198*, 82–87. https://doi.org/10.1046/j.1365-2818.2000.00710.x.

Gustafsson, M.G.L., Shao, L., Carlton, P.M., Wang, C.J.R., Golubovskaya, I.N., Cande, W.Z., Agard, D.A., and Sedat, J.W. (2008). Three-dimensional resolution doubling in wide-field fluorescence microscopy by structured illumination. Biophys. J. *94*, 4957–4970. https://doi.org/10.1529/biophysj.107.120345.

Harke, B., Keller, J., Ullal, C.K., Westphal, V., Schönle, A., and Hell, S.W. (2008). Resolution scaling in STED microscopy. Opt Express *16*, 4154–4162. https://doi.org/10.1364/OE.16.004154.

Hein, B., Willig, K.I., Wurm, C.A., Westphal, V., Jakobs, S., and Hell, S.W. (2010). Stimulated emission depletion nanoscopy of living cells

using SNAP-tag fusion proteins. Biophys. J. *98*, 158–163. https://doi.org/10.1016/j.bpj.2009.09.053.

Heine, J., Reuss, M., Harke, B., D'Este, E., Sahl, S.J., and Hell, S.W. (2017). Adaptive-illumination STED nanoscopy. Proc. Natl. Acad. Sci. USA *114*, 9797–9802. https://doi.org/10.1073/pnas.1708304114.

Hell, S.W., Dyba, M., and Jakobs, S. (2004). Concepts for nanoscale resolution in fluorescence microscopy. Curr. Opin. Neurobiol. *14*, 599–609. https://doi.org/10.1016/j.conb.2004.08.015.

Hell, S.W., Jakobs, S., and Kastrup, L. (2003). Imaging and writing at the nanoscale with focused visible light through saturable optical transitions. Appl. Phys. Mater. Sci. Process *77*, 859–860. https://doi.org/10.1007/s00339-003-2292-4.

Hell, S.W., and Wichmann, J. (1994). Breaking the diffraction resolution limit by stimulated emission: stimulated-emission-depletion fluorescence microscopy. Opt. Lett. *19*, 780–782. https://doi.org/10.1364/OL.19.000780.

Helmchen, F., and Denk, W. (2005). Deep tissue two-photon microscopy. Nat. Methods *2*, 932–940. https://doi.org/10.1038/nmeth818.

Herring, B.E., and Nicoll, R.A. (2016). Long-term potentiation: from CaMKII to AMPA receptor trafficking. Annu. Rev. Physiol. *78*, 351–365. https://doi.org/10.1146/annurev-physiol-021014-071753.

Herzog, E., Nadrigny, F., Silm, K., Biesemann, C., Helling, I., Bersot, T., Steffens, H., Schwartzmann, R., Nägerl, U.V., El Mestikawy, S., et al. (2011). In vivo imaging of intersynaptic vesicle exchange using VGLUT1Venus knock-in mice. J. Neurosci. *31*, 15544–15559. https://doi.org/10.1523/JNEUROSCI.2073-11.2011.

Hofmann, M., Eggeling, C., Jakobs, S., and Hell, S.W. (2005). Breaking the diffraction barrier in fluorescence microscopy at low light intensities by using reversibly photoswitchable proteins. Proc. Natl. Acad. Sci. USA *102*, 17565–17569. https://doi.org/10.1073/pnas.0506010102.

Holtmaat, A., Bonhoeffer, T., Chow, D.K., Chuckowree, J., De Paola, V., Hofer, S.B., Hübener, M., Keck, T., Knott, G., Lee, W.-C.A., et al. (2009). Long-term, high-resolution imaging in the mouse neocortex through a chronic cranial window. Nat. Protoc. *4*, 1128–1144. https://doi.org/10.1038/nprot.2009.89.

Holtmaat, A.J.G.D., Trachtenberg, J.T., Wilbrecht, L., Shepherd, G.M., Zhang, X., Knott, G.W., and Svoboda, K. (2005). Transient and persistent dendritic spines in the neocortex in vivo. Neuron *45*, 279–291. https://doi.org/10.1016/j.neuron.2005.01.003.

Jacques, S.L. (2013). Optical properties of biological tissues: a review. Phys. Med. Biol. *58*, R37–R61. https://doi.org/10.1088/0031-9155/58/11/R37.

Kilian, N., Goryaynov, A., Lessard, M.D., Hooker, G., Toomre, D., Rothman, J.E., and Bewersdorf, J. (2018). Assessing photodamage in live-cell STED microscopy. Nat. Methods *15*, 755–756. https://doi.org/10.1038/s41592-018-0145-5.

Kner, P., Chhun, B.B., Griffis, E.R., Winoto, L., and Gustafsson, M.G.L. (2009). Super-resolution video microscopy of live cells by structured illumination. Nat. Methods *6*, 339–342. https://doi.org/10.1038/nmeth.1324.

Koho, S.V., Slenders, E., Tortarolo, G., Castello, M., Buttafava, M., Villa, F., Tcarenkova, E., Ameloot, M., Bianchini, P., Sheppard, C.J.R., et al. (2020). Two-photon image-scanning microscopy with SPAD array and blind image reconstruction. Biomed. Opt Express *11*, 2905–2924. https://doi.org/10.1364/boe.374398.

Kumari, A., Kesarwani, S., Javoor, M.G., Vinothkumar, K.R., and Sirajuddin, M. (2020). Structural insights into actin filament recognition by commonly used cellular actin markers. EMBO J. *39*, e104006–13. https://doi.org/10.15252/embj.2019104006.

Laissue, P.P., Alghamdi, R.A., Tomancak, P., Reynaud, E.G., and Shroff, H. (2017). Assessing phototoxicity in live fluorescence imaging. Nat. Methods *14*, 657–661. https://doi.org/10.1038/nmeth.4344.

Langille, J.J., and Brown, R.E. (2018). The synaptic theory of memory: a historical survey and reconciliation of recent opposition. Front. Syst. Neurosci. *12*, 52. https://doi.org/10.3389/fnsys.2018.00052.

Li, D., Shao, L., Chen, B.C., Zhang, X., Zhang, M., Moses, B., Milkie, D.E., Beach, J.R., Hammer, J.A., Pasham, M., et al. (2015). Extended-resolution structured illumination imaging of endocytic and cytoskeletal dynamics. Science *349*, aab3500. https://doi.org/10.1126/science.aab3500.

Li, Z., Zhang, Q., Chou, S.W., Newman, Z., Turcotte, R., Natan, R., Dai, Q., Isacoff, E.Y., and Ji, N. (2020). Fast widefield imaging of neuronal structure and function with optical sectioning in vivo. Sci. Adv. *6*, eaaz3870–13. https://doi.org/10.1126/sciadv.aaz3870.

Lin, M.Z., McKeown, M.R., Ng, H.L., Aguilera, T.A., Shaner, N.C., Campbell, R.E., Adams, S.R., Gross, L.A., Ma, W., Alber, T., and Tsien, R.Y. (2009). Autofluorescent proteins with excitation in the optical window for intravital imaging in mammals. Chem. Biol. *16*, 1169–1179. https://doi.org/10.1016/j.chembiol.2009.10.009.

Lukinavičius, G., Reymond, L., D'Este, E., Masharina, A., Göttfert, F., Ta, H., Güther, A., Fournier, M., Rizzo, S., Waldmann, H., et al. (2014). Fluorogenic probes for live-cell imaging of the cytoskeleton. Nat. Methods *11*, 731–733. https://doi.org/10.1038/nmeth.2972.

Lukosz, W., and Marchand, M. (1963). Optischen abbildung unter überschreitung der Beugungsbedingten auflösungsgrenze. Opt. Acta *10*, 241–255. https://doi.org/10.1080/713817795.

Markwirth, A., Lachetta, M., Mönkemöller, V., Heintzmann, R., Hübner, W., Huser, T., and Müller, M. (2019). Video-rate multi-color structured illumination microscopy with simultaneous real-time reconstruction. Nat. Commun. *10*, 4315–4411. https://doi.org/10.1038/s41467-019-12165-x.

Masch, J.-M., Steffens, H., Fischer, J., Engelhardt, J., Hubrich, J., Keller-Findeisen, J., D'Este, E., Urban, N.T., Grant, S.G.N., Sahl, S.J., et al. (2018). Robust nanoscopy of a synaptic protein in living mice by organic-fluorophore labeling. Proc. Natl. Acad. Sci. USA *115*, E8047–E8056. https://doi.org/10.1073/pnas.1807104115.

Masullo, L.A., Bodén, A., Pennacchietti, F., Coceano, G., Ratz, M., and Testa, I. (2018). Enhanced photon collection enables four dimensional fluorescence nanoscopy of living systems. Nat. Commun. *9*, 3281. https://doi.org/10.1038/s41467-018-05799-w.

May, M.A., Barré, N., Kummer, K.K., Kress, M., Ritsch-Marte, M., and Jesacher, A. (2021). Fast holographic scattering compensation for deep tissue biological imaging. Nat. Commun. *12*, 4340. https://doi.org/10.1038/s41467-021-24666-9.

Moneron, G., and Hell, S.W. (2009). Two-photon excitation STED microscopy. Opt Express *17*, 14567–14573. https://doi.org/10.1364/oe.17.014567.

Müller, C.B., and Enderlein, J. (2010). Image scanning microscopy. Phys. Rev. Lett. *104*, 198101–198104. https://doi.org/10.1103/PhysRevLett.104.198101.

Nägerl, U.V., Willig, K.I., Hein, B., Hell, S.W., and Bonhoeffer, T. (2008). Live-cell imaging of dendritic spines by STED microscopy. Proc. Natl. Acad. Sci. USA *105*, 18982–18987. https://doi.org/10.1073/pnas.0810028105.

Neil, M.A.A., Juškaitis, R., and Wilson, T. (1998). Real time 3D fluorescence microscopy by two beam interference illumination. Opt Commun. *153*, 1–4. https://doi.org/10.1016/S0030-4018(98)00210-7.

Neil, M.A., Juškaitis, R., and Wilson, T. (1997). Method of obtaining optical sectioning by using structured light in a conventional microscope. Opt. Lett. *22*, 1905–1907. https://doi.org/10.1364/OL.22.001905.

Papadopoulos, I.N., Jouhanneau, J.S., Poulet, J.F.A., and Judkewitz, B. (2017). Scattering compensation by focus scanning holographic aberration probing (F-SHARP). Nat. Photonics *11*, 116–123. https://doi.org/10.1038/nphoton.2016.252.

Park, J.H., Sun, W., and Cui, M. (2015). High-resolution in vivo imaging of mouse brain through the intact skull. Proc. Natl. Acad. Sci. USA *112*, 9236–9241. https://doi.org/10.1073/pnas.1505939112.

J.B. Pawley, ed. (2006). Handbook Of Biological Confocal Microscopy (Boston, MA: Springer US). https://doi.org/10.1007/978-0-387-45524-2.

Pfeiffer, T., Poll, S., Bancelin, S., Angibaud, J., Inavalli, V.K., Keppler, K., Mittag, M., Fuhrmann, M., and Nägerl, U.V. (2018). Chronic 2P-STED imaging reveals high turnover of dendritic spines in the hippocampus in vivo. Elife *7*. e34700–17. https://doi.org/10.7554/eLife.34700.

Pozzi, P., Gandolfi, D., Porro, C.A., Bigiani, A., and Mapelli, J. (2020). Scattering compensation for deep brain microscopy: the long road to get proper images. Front. Phys. *8*, 1–6. https://doi.org/10.3389/fphy.2020.00026.

Riedl, J., Crevenna, A.H., Kessenbrock, K., Yu, J.H., Neukirchen, D., Bista, M., Bradke, F., Jenne, D., Holak, T.A., Werb, Z., et al. (2008). Lifeact: a

versatile marker to visualize F-actin. Nat. Methods *5*, 605–607. https://doi.org/10.1038/nmeth.1220.

Sahl, S.J., Schönle, A., and Hell, S.W. (2019). In Fluorescence Microscopy with Nanometer Resolution, P.W. Hawkes and J.C.H. Spence, eds. (Cham: Springer International Publishing), pp. 1089–1143. https://doi.org/10.1007/978-3-030-00069-1_22.

Schulz, O., Pieper, C., Clever, M., Pfaff, J., Ruhlandt, A., Kehlenbach, R.H., Wouters, F.S., Großhans, J., Bunt, G., and Enderlein, J. (2013). Resolution doubling in fluorescence microscopy with confocal spinning-disk image scanning microscopy. Proc. Natl. Acad. Sci. USA *110*, 21000–21005. https://doi.org/10.1073/pnas.1315858110.

Sheppard, C.J.R. (2021a). Structured illumination microscopy and image scanning microscopy: a review and comparison of imaging properties. Philos. Trans. A Math. Phys. Eng. Sci. *379*, 20200154. https://doi.org/10.1098/rsta.2020.0154.

Sheppard, C.J.R. (2021b). The development of microscopy for super-resolution: confocal microscopy, and image scanning microscopy. Appl. Sci. *11*, 8981. https://doi.org/10.3390/app11198981.

Sheppard, C.J.R. (1987). Super-resolution in confocal imaging. In Optik (Jena), H.H. Arsenault, ed., p. 161.

Sheppard, C.J.R., Mehta, S.B., and Heintzmann, R. (2013). Superresolution by image scanning microscopy using pixel reassignment. Opt. Lett. *38*, 2889–2892. https://doi.org/10.1364/ol.38.002889.

Staudt, T., Engler, A., Rittweger, E., Harke, B., Engelhardt, J., and Hell, S.W. (2011). Far-field optical nanoscopy with reduced number of state transition cycles. Opt Express *19*, 5644–5657. https://doi.org/10.1364/OE.19.005644.

Steffens, H., Mott, A.C., Li, S., Wegner, W., Švehla, P., Kan, V.W.Y., Wolf, F., Liebscher, S., and Willig, K.I. (2021). Stable but not rigid: chronic in vivo STED nanoscopy reveals extensive remodeling of spines, indicating multiple drivers of plasticity. Sci. Adv. *7*, eabf2806. https://doi.org/10.1126/sciadv.abf2806.

Steffens, H., Wegner, W., and Willig, K.I. (2020). In vivo STED microscopy: a roadmap to nanoscale imaging in the living mouse. Methods *174*, 42–48. https://doi.org/10.1016/j.ymeth.2019.05.020.

Svoboda, K., and Yasuda, R. (2006). Principles of two-photon excitation microscopy and its applications to neuroscience. Neuron *50*, 823–839. https://doi.org/10.1016/j.neuron.2006.05.019.

Tang, A.-H., Chen, H., Li, T.P., Metzbower, S.R., MacGillavry, H.D., and Blanpied, T.A. (2016). A trans-synaptic nanocolumn aligns neurotransmitter release to receptors. Nature *536*, 210–214. https://doi.org/10.1038/nature19058.

Tang, J., Germain, R.N., and Cui, M. (2012). Superpenetration optical microscopy by iterative multiphoton adaptive compensation technique. Proc. Natl. Acad. Sci. USA *109*, 8434–8439. https://doi.org/10.1073/pnas.1119590109.

Testa, I., Urban, N.T., Jakobs, S., Eggeling, C., Willig, K.I., and Hell, S.W. (2012). Nanoscopy of living brain slices with low light levels. Neuron *75*, 992–1000. https://doi.org/10.1016/j.neuron.2012.07.028.

Tønnesen, J., Inavalli, V.V.G.K., and Nägerl, U.V. (2018). Super-resolution imaging of the extracellular space in living brain tissue. Cell *172*, 1108–1121.e15. https://doi.org/10.1016/j.cell.2018.02.007.

Traenkle, B., and Rothbauer, U. (2017). Under the microscope: single-domain antibodies for live-cell imaging and super-resolution microscopy. Front. Immunol. *8*, 1030–1038. https://doi.org/10.3389/fimmu.2017.01030.

Turcotte, R., Liang, Y., Tanimoto, M., Zhang, Q., Li, Z., Koyama, M., Betzig, E., and Ji, N. (2019). Dynamic super-resolution structured illumination imaging in the living brain. Proc. Natl. Acad. Sci. USA *116*, 9586–9591. https://doi.org/10.1073/pnas.1819965116.

Urban, B.E., Xiao, L., Dong, B., Chen, S., Kozorovitskiy, Y., and Zhang, H.F. (2018). Imaging neuronal structure dynamics using 2-photon super-resolution patterned excitation reconstruction microscopy. J. Biophotonics *11*. e201700171–9. https://doi.org/10.1002/jbio.201700171.

Urban, B.E., Yi, J., Chen, S., Dong, B., Zhu, Y., Devries, S.H., Backman, V., and Zhang, H.F. (2015). Super-resolution two-photon microscopy via scanning patterned illumination. Phys. Rev. E Stat. Nonlin. Soft Matter Phys. *91*, 042703–042706. https://doi.org/10.1103/PhysRevE.91.042703.

Velasco, M.G.M., Zhang, M., Antonello, J., Yuan, P., Allgeyer, E.S., May, D., M'Saad, O., Kidd, P., Barentine, A.E.S., Greco, V., et al. (2021). 3D super-resolution deep-tissue imaging in living mice. Optica *8*, 442–450. https://doi.org/10.1364/optica.416841.

Vellekoop, I.M., and Mosk, A.P. (2007). Focusing coherent light through opaque strongly scattering media. Opt. Lett. *32*, 2309–2311. https://doi.org/10.1364/ol.32.002309.

Wagner, T.R., and Rothbauer, U. (2020). Nanobodies right in the MIDDLE: INTRABODIES as toolbox to visualize and modulate antigens in the living cell. Biomolecules *10*, E1701–E1719. https://doi.org/10.3390/biom10121701.

Wang, J., and Zhang, Y. (2021). Adaptive optics in super-resolution microscopy. Biophys. Rep. *7*, 267–279. https://doi.org/10.52601/bpr.2021.210015.

Wegner, W., Ilgen, P., Gregor, C., van Dort, J., Mott, A.C., Steffens, H., and Willig, K.I. (2017). In vivo mouse and live cell STED microscopy of neuronal actin plasticity using far-red emitting fluorescent proteins. Sci. Rep. *7*, 11781. https://doi.org/10.1038/s41598-017-11827-4.

Wegner, W., Mott, A.C., Grant, S.G.N., Steffens, H., and Willig, K.I. (2018). In vivo STED microscopy visualizes PSD95 sub-structures and morphological changes over several hours in the mouse visual cortex. Sci. Rep. *8*, 219. https://doi.org/10.1038/s41598-017-18640-z.

Wegner, W., Steffens, H., Gregor, C., Wolf, F., and Willig, K.I. (2022). Environmental enrichment enhances patterning and remodeling of synaptic nanoarchitecture as revealed by STED nanoscopy. Elife *11*. 2020.10.23.352195. https://doi.org/10.7554/eLife.73603.

Willig, K.I., Kellner, R.R., Medda, R., Hein, B., Jakobs, S., and Hell, S.W. (2006). Nanoscale resolution in GFP-based microscopy. Nat. Methods *3*, 721–723. https://doi.org/10.1038/nmeth922.

Willig, K.I., Steffens, H., Gregor, C., Herholt, A., Rossner, M.J., and Hell, S.W. (2014). Nanoscopy of filamentous actin in cortical dendrites of a living mouse. Biophys. J. *106*, L01–L03. https://doi.org/10.1016/j.bpj.2013.11.1119.

Willig, K.I., Wegner, W., Müller, A., Calvet-Fournier, V., and Steffens, H. (2021). Multi-label in vivo STED microscopy by parallelized switching of reversibly switchable fluorescent proteins. Cell Rep. *35*, 109192. https://doi.org/10.1016/j.celrep.2021.109192.

Winter, P.W., York, A.G., Nogare, D.D., Ingaramo, M., Christensen, R., Chitnis, A., Patterson, G.H., and Shroff, H. (2014). Two-photon instant structured illumination microscopy improves the depth penetration of super-resolution imaging in thick scattering samples. Optica *1*, 181–191. https://doi.org/10.1364/optica.1.000181.

York, A.G., Chandris, P., Nogare, D.D., Head, J., Wawrzusin, P., Fischer, R.S., Chitnis, A., and Shroff, H. (2013). Instant super-resolution imaging in live cells and embryos via analog image processing. Nat. Methods *10*, 1122–1126. https://doi.org/10.1038/nmeth.2687.

York, A.G., Parekh, S.H., Dalle Nogare, D., Fischer, R.S., Temprine, K., Mione, M., Chitnis, A.B., Combs, C.A., and Shroff, H. (2012). Resolution doubling in live, multicellular organisms via multifocal structured illumination microscopy. Nat. Methods *9*, 749–754. https://doi.org/10.1038/nmeth.2025.

Yu, D., Lee, H., Hong, J., Jung, H., Jo, Y., Oh, B.H., Park, B.O., and Heo, W.D. (2019). Optogenetic activation of intracellular antibodies for direct modulation of endogenous proteins. Nat. Methods *16*, 1095–1100. https://doi.org/10.1038/s41592-019-0592-7.

Zheng, X., Zhou, J., Wang, L., Wang, M., Wu, W., Chen, J., Qu, J., Gao, B.Z., and Shao, Y. (2021). Current challenges and solutions of super-resolution structured illumination microscopy. APL Photonics *6*, 020901. https://doi.org/10.1063/5.0038065.